Radiation effects of CERN-PS 24 GeV/c protons in ATLAS18 ITk strip sensors

I. Mandić[a,*], V. Cindro[a], M. Mikuž[a,b], B. Novak[a], P. Federičová[c], R. Jirásek[c], J. Kroll[c], J. Kvasnička[c], M. Mikeštíková[c], P. Tůma[c], V. Fadeyev[d], Y. Unno[e], E. Bach[f], C. Fleta[f], M. Ullan[f], U. Soldevila[g], R.S. Orr[h], C.K. Mahajan[h], S.K. Sridhar[h], A. S. Chisholm[i], I. Dawson[j]

[a]*Jožef Stefan Institute, Jamova 39, 1000, Ljubljana, Slovenia*
[b]*Faculty of Mathematics and Physics, University of Ljubljana , Jadranska ulica 19, 1000, Ljubljana, Slovenia*
[c]*Institute of Physics, Academy of Sciences of the Czech Republic, Na Slovance 2, 18200, Prague 8, Czech Republic*
[d]*Santa Cruz Institute for Particle Physics (SCIPP), University of California, Santa Cruz, CA 95064, USA*
[e]*Institute of Particle and Nuclear Study, High Energy Accelerator Research Organization (KEK), 1-1 Oho, Tsukuba, Ibaraki 305-0801, Japan*
[f]*Instituto de Microelectrónica de Barcelona (IMB-CNM), CSIC, Campus UAB-Bellaterra, 08193, Barcelona, Spain*
[g]*Instituto de Física Corpuscular, IFIC/CSIC-UV, C/Catedrático José Beltrán 2, E-46980, Paterna, Valencia, Spain*
[h]*Department of Physics, University of Toronto, 60 Saint George St., Toronto, Ontario M5S1A7, Canada*
[i]*School of Physics and Astronomy, University of Birmingham, Birmingham, B1 52TT, United Kingdom*
[j]*Particle Physics Research Centre, Queen Mary University of London, G.O. Jones Building, Mile End Road, London, E1 4NS, United Kingdom*

Abstract

Test structures from ATLAS ITk strip detector wafers were irradiated with 24 GeV/c protons. Samples were positioned at various angles with respect

───────────────

*Corresponding author

Email address: `igor.mandic@ijs.si` (I. Mandić)

to the proton beam. Blocks of G10 material were placed in front of detectors to study the effect of scattering of primary protons on fluence received by samples. Results confirm that both angle and scattering have a significant effect on the actual fluence to which samples are exposed. Miniature strip detectors irradiated with protons were also irradiated with reactor neutrons so that the combination of equivalent fluences from protons and neutrons matched the combination expected in the most exposed part in ITk strip detector. Good charge collection was measured confirming that strip detectors in ATLAS ITk are sufficiently radiation hard for successful operation up to highest fluences expected at HL-LHC.

1. Introduction

Silicon strip detectors in the Inner Tracker (ITk) [1, 2] of the upgraded ATLAS experiment at HL-LHC will have to operate in high radiation environments. Strip sensor region of the tracker is designed to withstand irradiation with 1 MeV neutron equivalent fluence of $1.6 \cdot 10^{15}$ n_{eq}/cm^2. To achieve such radiation hardness, extensive irradiation studies were performed during development of sensors. These included irradiations with reactor neutrons as well as low (25 MeV and 70 MeV kinetic energy) and high (24 GeV/c momentum) energy protons. During four years of production of more than 25000 sensors for the ITk, regular irradiations of test structures with neutrons and low energy protons are a part of production quality assurance (QA) procedures [3]. Because of less frequent availability, irradiations with high energy protons are not part of QA, but irradiation campaigns with 24 GeV/c pro-

2

tons at CERN PS were carried out to check the effect of high energy hadrons on samples from production wafers. This is important because the balance of ionizing dose and bulk damage of protons at this energy is the closest to the one expected in the experiment from all sources. In ATLAS experiment displacement damage to strip detectors will be caused by charged hadrons and neutrons. In the most exposed part of ITk strip detector charged hadrons and neutrons will contribute roughly equally to the Non Ionizing Energy Loss (NIEL) while in other regions neutrons will dominate.

After initial irradiation tests of mini strip sensors with 24 GeV/c protons Collected Charge (CC) was significantly lower than expected in certain range of fluences [2]. This initiated extensive irradiation, measurement and simulation work which will be described in the next sections.
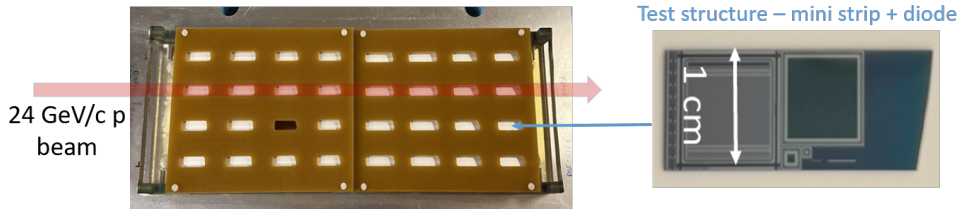
2. Experimental setup

Figure 1: Photo of the mechanical support used in irradiations is shown on the left. Test structure called mini&MD8 on the right contains a mini strip detector (1 cm x 1 cm) and a diode (0.8 cm x 0.8 cm). Test structures were placed in holders in the support structure machined in the 6 mm thick G10 material.

Irradiations with 24 GeV/c protons were done at IRRAD test facility at

---

[2]See the section 6, and Figure 9.

CERN [4, 5]. Proton beam at IRRAD is narrow with a roughly Gaussian shape of beam intensity profile with $\text{FWHM}_x = 7.8$ mm and $\text{FWHM}_y = 9.7$ mm determined with Beam Profile Monitor [4, 5]. No scanning of samples was provided in the facility. Test structures used in these studies were taken from the ITk strip sensor production ATLAS18 wafers [3, 6, 7]. The structure called mini&MD8 contains a mini strip detector and a pad diode on a single piece of silicon with size of roughly 1x2 cm^2 - see Fig. 1. To irradiate a structure of this size, without scanning, it was placed in the narrow beam at shallow angle of $\sim 2.3°$. Support for the test structures was made of G10 material in which place holders were machined as shown in Fig. 1. Several samples were placed one behind the other in the beam direction and irradiated together with the same beam (see Fig. 1) which resulted in thick layers of G10 and silicon materials on which primary protons scattered and generated showers of secondary particles. As mentioned above, lower than expected charge collection efficiency was measured with mini strip detectors irradiated in the described setup and simulations indicated that the reason might have been the increase of effective fluence due to secondary particles originating from G10 or/and silicon of irradiated devices because of their shallow angle and therefore long proton path in silicon.

To study the effects of angle and scattering a different experimental setup was built, as shown in Figure 2. Samples - mini strip detectors, test chips containing various test circuits and pad diodes [6] - were cut to 1×1 cm^2 size from the larger ITk strip test structures (see [7] and Fig. 1) and fixed to light weight holders made of thin layer of plastic, PEEK (PolyEther Ether Ketone). Twelve holders, each holding samples on both sides of the holder
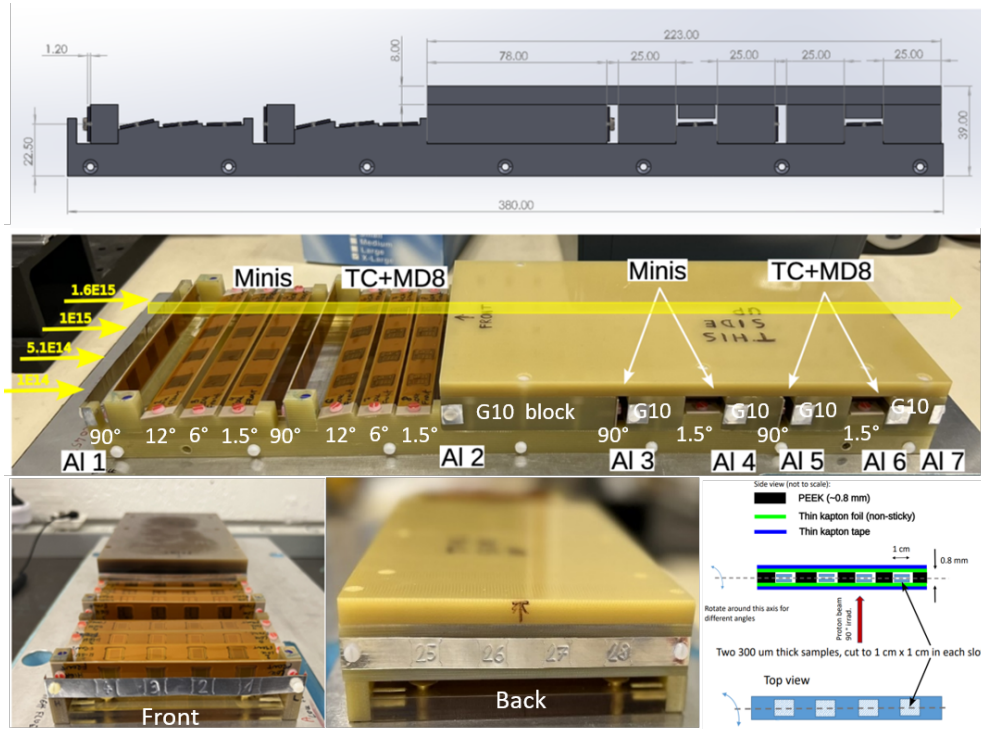
4

Figure 2: Drawing of side view and photos of the irradiation setup for study of effects of angle and scattering. Pairs of Mini strip (Minis) detectors were mounted on the first four light weight holders and pairs of one Test Chip and one MD8 diode (TC+MD8) on next four holders. Holders were positioned at different angles with respect to the beam direction. Test structures were placed also behind blocks of G10 material to study the effect of scattering of proton beam. Seven layers of aluminium foils were mounted in the setup for monitoring of proton fluence.

at four positions were mounted at different angles to the direction of the proton beam as shown in Fig. 2. Two sets of four holders were mounted at angles 90°, 12°, 6°, 1.5°. First set contained pairs of mini strip sensors on each side of the holder and the second set a Test Chips (TC) on one side and a MD8 pad diode on the other. Blocks of G10 material were placed in

5

front of last 4 holders mounted at 90° and 1.5°. Samples were aligned in 4 columns separated by 2.4 cm. Each of the columns was centred in the proton beam and kept at fixed position (there was no scanning) during irradiation. Fluence delivered to samples in neighbouring columns could be neglected. After irradiation of one column was finished, next column was moved into the beam. Target fluences were $1 \cdot 10^{14}$, $5 \cdot 10^{14}$, $1 \cdot 10^{15}$ and $1.6 \cdot 10^{15}$ n_{eq}/cm^2. Sample holder was placed in the cold box maintaining temperature during irradiation at -20°C.

3. Dosimetry and simulation

Proton fluence was monitored by measuring activity of ^{22}Na and ^{24}Na in aluminium (Al) foils [8]. As shown in Fig. 2, 7 layers of Al foils were installed in the setup. After irradiation 1×1 cm^2 pieces matching the positions of columns of samples were cut from Al foils and their radioactivity measured with accuracy of 7%. Proton fluence taken from the activated foil dosimetry is converted to 1 MeV neutron equivalent fluence in silicon by multiplying it with the hardness factor of 0.62 [9]. Figure 3a shows 1 MeV neutron equivalent fluences measured with 7 layers of Al foils for 4 target fluences (i.e. columns in the setup). It can be seen in Fig. 3a that there are significant differences between target and delivered fluences measured with Al foil on layer 1, especially for the two higher fluences. The differences arose because irradiation was stopped before target fluences were reached. But the striking feature of Fig. 3a is the significant increase of measured fluence on layer 2 and especially on layer 3 behind the first G10 scattering block in the setup caused by scattering of beam on material in the setup - see Figure 2.

6
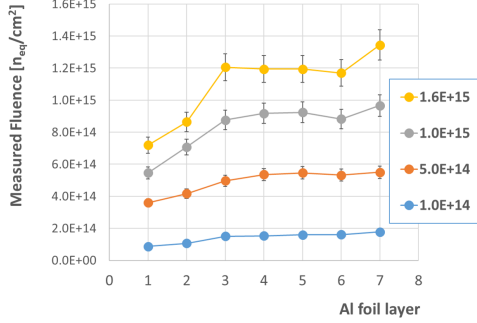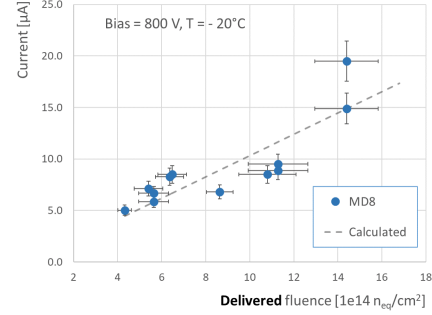
Figure 3: Figure a) shows fluences measured with 28 aluminium pieces for four columns corresponding to target fluences written in the figure. Figure b) shows current measured with MD8 diodes vs. fluence measured with Al foils. Dashed line shows calculated current vs. fluence for fully depleted MD8 diode.

MD8 structures irradiated in the setup (see Fig. 2) are silicon pad diodes with 0.8×0.8 cm^2 surface, 320 μm thick . Reverse current vs. bias voltage was measured with these diodes irradiated in $5.1 \cdot 10^{14}$ and $1.6 \cdot 10^{15}$ n$_{eq}$/cm^2 target fluence columns. Current was measured after annealing at 60°C for 80 minutes. Figure 3b shows current at 800 V reverse bias as the function of delivered fluence according to Table 1 together with current calculated for fully depleted diode $I = \alpha \cdot \Phi_{eq} \cdot V$ where $\alpha = 4 \cdot 10^{-17}$ Acm^{-1} at 20°C is the reverse current scaling factor [10], Φ_{eq} is equivalent fluence and V is depleted volume. Bias of 800 V was chosen because diodes were fully depleted below this voltage also at highest fluences. A reasonable agreement between calculated and measured current can be seen. This provides a degree of confidence that Al activation is still a reasonable measure of fluence even when secondary particles are involved (e.g. pions, neutrons, protons). These

7

secondaries are mainly created in inelastic collisions between the high-energy proton beam and atomic nuclei in the support material. However, to fully understand the relationship between activation and fluence in this radiation environment, dedicated particle transport simulation studies will be needed.

Geant4 simulation [11] of the experiment was made using the Shielding physics lilst [12] and compared with Al dosimetry. Detailed CAD drawing of the irradiation setup in Fig. 2 was used to describe the material distribution in the simulation as shown in Fig. 4a. NIEL in mini strip detectors was calculated by summing the path lengths of particles in Si and using the damage factors. Fluences relative to the fluence in layer 1 calculated in Geant4 simulation are shown in Fig. 4b together with measured relative fluences. Points are averages for four foils at each layer and error bars show standard deviation of these four values. It can be seen that at layer 3 fluence is 60% larger than at layer 1 which is a large effect. There is good agreement between measurement and simulation for layer 2 while for higher layer numbers simulation underestimates measured values to some extent. It should be noted that only rough agreement is expected, despite the precise material distribution, due to a combination of factors, such as the true beam shape deviating from the Gaussian function used in the simulation. Differences could be caused also by imperfections of alignment with the beam which are not included in simulation. The uncertainty of correlation between aluminium foil activation and fluence in environment with secondary particles may also play a significant role in these discrepancies. Further studies would be needed to improve the understanding of these effects.

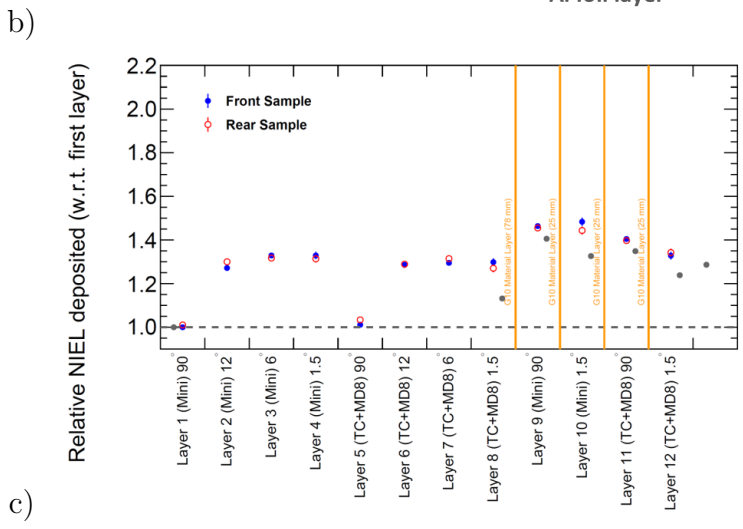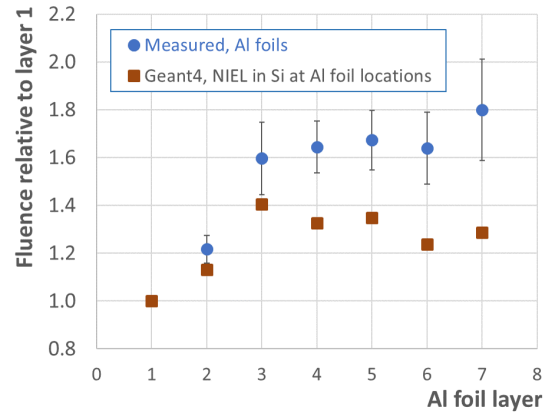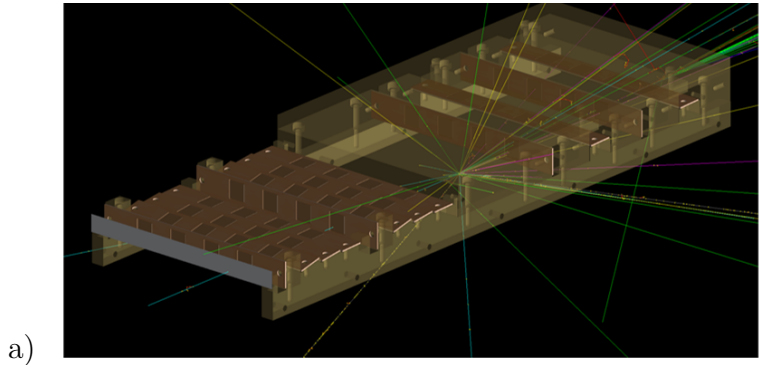Figure 4c) shows Geant4 relative fluences for silicon samples and alu-

8

a)

b)

c)

Figure 4: Figure a) shows the drawing of the setup used in Geant4 simulation with an event showing secondary tracks generated at an interaction of primary proton. Figure b) shows fluence relative to measured with Al foil in layer 1 and relative fluences calculated with Geant4 simulation. Measured values are averages for the measurements of four fluences per layer and error bars show standard deviation of the four measurements. Figure c) shows relative fluences calculated by Geant4 simulation for silicon samples at different layers. Fluence was calculated separately for two silicon samples at each position. Fluences calculated at locations of Al foils are indicated with grey symbols.

9

minium foils in the setup. It can be seen that the fluence for samples irradiated at shallow angles is significantly larger than the fluence of samples irradiated at 90°. This is geometrical effect because the FWHM of beam intensity profile is comparable with dimension of samples. At shallow angle a larger part of the sample is exposed to high intensity core of the beam than in case of exposure at 90°.

The effect of irradiation at shallow angle was studied also in a separate irradiation experiment at CERN IRRAD facility in which aluminium foils were irradiated at 90° and at 0°. The scheme of the experiment is shown in Fig. 5. Dimension of foil F1 was 0.5×0.5 cm^2 while foils F2 and F3 were 1×1 cm^2. Fluence measured in the small foil F1 was 70% larger than in the foil F2 at 90° while fluence in the horizontal foil F3 was 30% larger than fluence measured with F2. These signifiant differences between foils are the consequence of geometrical effects in the sharp proton beam.

The effect of angle is much less significant for samples with G10 scattering blocks between the beam and samples. This may be expected because the generation of secondaries from inelastic interactions creates many particles at large angles and therefore effectively broadens the beam size and so reduces the geometrical effect of shallow angle.

As shown in Fig. 2 Al foils were not near positions of all mini strip or MD8 samples so the true fluence to which samples were exposed was estimated based on measurements and simulation. Fluence measured with Al1 is the best estimate for actual fluence for samples in Layer 1 and this value was used also for layer 5 (90°), because Geant4 simulation also didn't show significant differences between these two layers. As mention above,
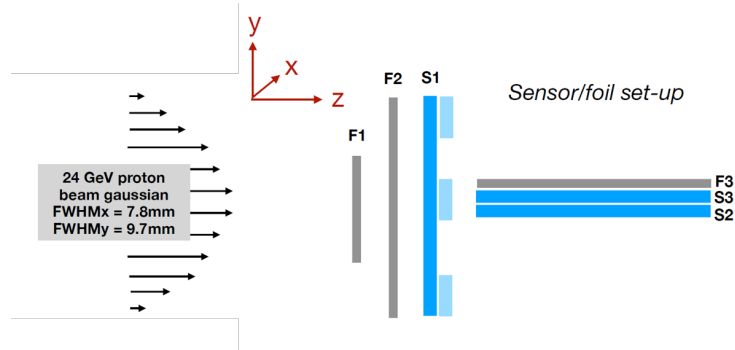
10

Figure 5: Scheme of the irradiation experiment. Mini strip sensors are marked with S and aluminium foils with F. Size of foil F1 is 0.5×0.5 cm^2 while F2 and F3 are 1×1 cm^2. The drawing is not to scale.

precision of fluence measurement with Al foil is 7%.

Simulation in Fig. 4c shows that devices irradiated at shallow angles in layers 2,3,4 and 6,7,8 were exposed to about 30% higher fluence than those in layer 1. The increase of fluence by 30% was seen also in the measurement shown in Fig. 5. Therefore, actual fluences for sensors in these layers were estimated by multiplying the fluence of layer 1 with factors calculated in Geant4 simulation. The uncertainty of this factor is estimated to be of the order of 10% and arises from the imperfect beam description in the simulation.

Sensors in layers behind G10 scattering blocks have aluminium layers in their vicinity. Al3 is near sensor layer 9, Al4 near layer 10, Al5 near layer 11 and Al6 near the last layer 12 (see Figures 2a and 4c). Fluences measured with these foils are taken as the estimates of actual fluences for the closest sensor layer. Aluminium foils were irradiated at 90° while sensors in layers 10 and 12 were at 1.5°. But as mentioned, simulation in Fig. 4c shows

that the effect of angle is significantly smaller than for layers without G10 material. Geant 4 simulation shows differences between fluences of sensors 9,10,11 and 12 and corresponding aluminium foils. The accuracy of delivered fluences was estimated from these differences. Delivered (actual) fluences for individual samples in 12 layers and 4 target fluences are summarized in Table 1.

Sensor layer	Angle [°]	Target 1e14	Target 5.1e14	Target 10e14	Target 16e14	Uncert.
1,5	90	0.9e14	3.6e14	5.5e14	7.2e14	7%
2,6	12	1.1e14	4.5e14	6.8e14	9.0e14	12%
3,4	6	1.1e14	4.7e14	7.1e14	9.4e14	12%
7,8	1.5	1.1e14	4.7e14	7.1e14	9.4e14	12%
9	90	1.5e14	5.0e14	8.8e14	12e14	10%
10	1.5	1.5e14	5.4e14	9.2e14	12e14	10%
11	90	1.6e14	5.4e14	9.2e14	12e14	10%
12	1.5	1.6e14	5.3e14	8.8e14	12e14	10%

Table 1: Table of delivered fluences.

4. Charge Collection measurements

Charge collection was measured with electrons from ^{90}Sr source with Alibava multi channel readout system using Beetle chip [13]. Mini strip detector was placed between ^{90}Sr source and a scintillator coupled to a photomultiplier. Trigger was provided by the signal from the scintillator generated by electron from ^{90}Sr that crossed the strip detector. Trigger arrival time with

respect to the Beetle clock was recorded with precision of 1 ns and only events from optimal, 10 ns wide, time window were selected for measurement of collected charge. Passage of electrons can induce signal in several neighbouring strips so the collected charge in an event was determined using a clustering algorithm. The distribution of cluster charges from several thousands of events was fitted with a Landau function convoluted with a Gaussian and the most probable value of Landau function was defined as the collected charge at given bias voltage. The uncertainty of collected charge estimated in this ways is about 1000 electrons [14]. Charge collection measurements shown in this work were made after annealing for 80 minutes at 60°C. See [15, 16] for more detail about measurement setup.

Figure 6 shows collected charge at 500 V measured with mini strip detectors irradiated at different angles with or without blocks of G10 material in the beam as a function of fluence. The bias of 500 V was chosen because this is the maximal bias voltage that can be applied to sensors in the ITk and 6350 electrons is defined as the minimum required charge collection after irradiation with $\Phi_{eq} = 1.6 \cdot 10^{15}$ n_{eq}/cm^2 - the so called QA acceptance level [7]. It can be seen in Figure 6 that collected charge is well above the QA acceptance level at all fluences of this experiment. The dependence of collected charge on fluence is comparable with previous experiments [15] but with significant spread. It should be noted that the beam in IRRAD is very sharp so that even the mini strip detectors are not irradiated uniformly and effective fluence may also depend on the position of the ^{90}Sr source, scintillator and collimators in experimental setups. This uncertainty was not included when estimating the accuracy of delivered fluences.
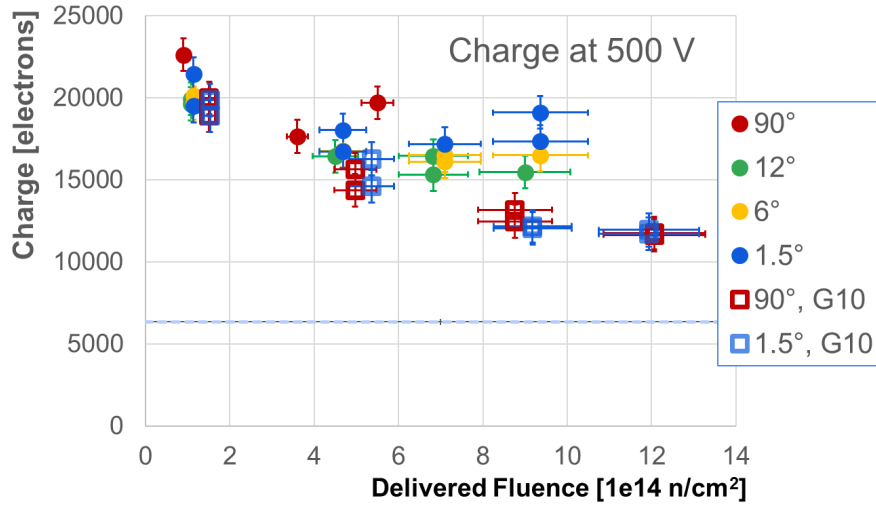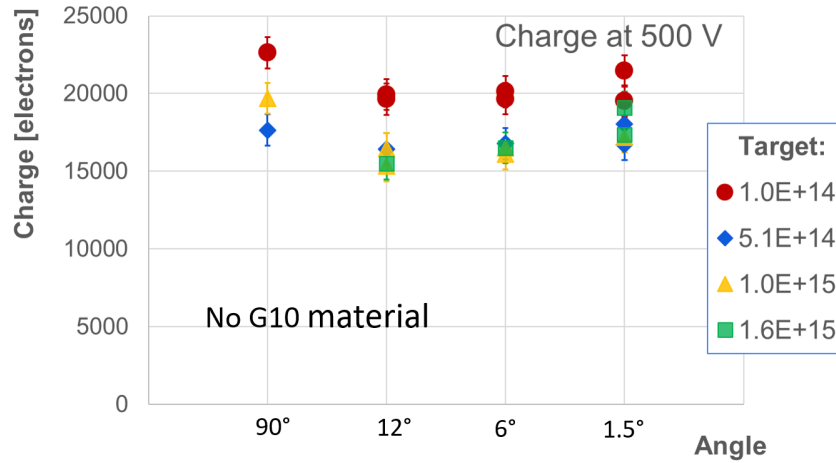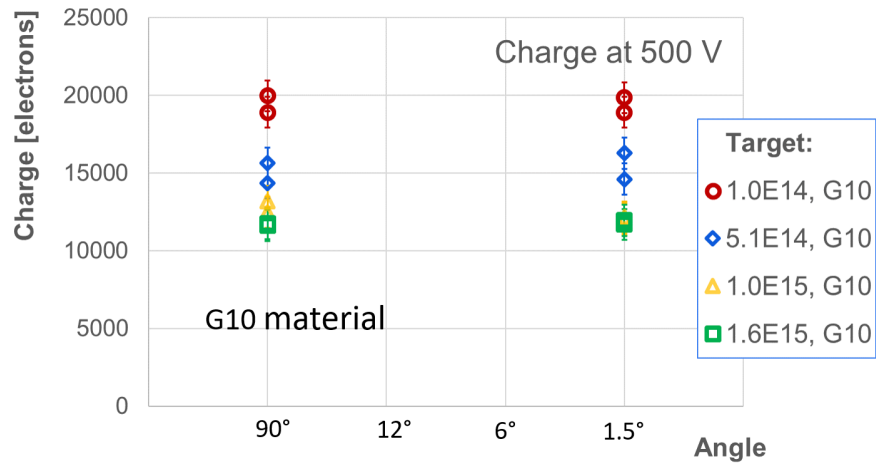
Figure 6: Figure shows collected charge at 500 V bias as vs. fluence measured with Al foils. Different symbols and colours represent sensors at different angles in front of or behind blocks of G10 material. Horizontal dashed line shows 6350 electrons charge which is the QA acceptance level.

Dependence on collected charge on irradiation angle is shown in Fig. 7. It can be seen that collected charge for sensors with no G10 material between the samples and the beam is higher at 90° than at shallower angles for any fluence. This is expected due to geometrical effect in a beam with Gaussian shape of beam profile with FWHM comparable to the dimension of the sample as explained before. It can be seen that for angles 12° and lower collected charge is slightly increasing as the angle drops. This effect is currently not understood and parameters like proton beam profile, details of position of samples in the beam should be known better to explain the feature.

14

a)

b)

Figure 7: Figure a) shows collected charge vs. angle for sensor layers 1, 2, 3 and 4, without G10 material between the beam and sensors. Different colours are for different target fluences (i.e. columns in the setup). In figure b) collected charge measured with sensors at 90° and 1.5° in layers 9 and 10, with G10 material in the beam.

15

For sensors with G10 material between the beam and the samples shown in Fig. 7b no dependence on angle is observed. The explanation for this may be that secondary particles which increase the effective fluence by about 60% (see Fig. 4b) are generated at larger angles and so make the effective beam less sharp and irradiation more uniform thus reducing the influence of angle. Geant4 simulation in Fig. 4c also showed much smaller effect of angle for sensors in layers 9,10 than for layers 1,2,3 and 4.

Measurements shown in this section confirm that material of the support structure and irradiation at shallow angle can cause a significant increase of effective fluence which results in significantly lower collected charge. It is therefore very likely that these effects contributed to low values of collected charge measured in some of previous irradiations at IRRAD facility.

5. Mixed Irradiation

In upgraded ATLAS experiment silicon strip detectors will be exposed to a mixture of neutrons and high energy charged hadrons [2]. More than 50% of displacement damage in silicon strip detectors will be caused by neutrons and the rest by charged hadrons. In the most exposed part, ITk strip detectors will accumulate $\Phi_{eq} \sim 5 \cdot 10^{14}$ n_{eq}/cm^2 from charged hadrons while displacement damage equivalent to fluence $\Phi_{eq} \sim 6 \cdot 10^{14}$ n_{eq}/cm^2 will come from neutrons. These are expected radiation levels after 4000 fb^{-1}. Strip detectors were designed with a safety factor of 1.5 for total fluence of $\Phi_{eq} = 1.6 \cdot 10^{15}$ n_{eq}/cm^2 of which $\Phi_{eq} \sim 7 \cdot 10^{14}$ n_{eq}/cm^2 comes from charged hadrons and $\Phi_{eq} \sim 9 \cdot 10^{14}$ n_{eq}/cm^2 from neutrons.

To check the performance of detector after irradiation with a mixture of

particles, a sample that was exposed to $\Phi_{eq} \sim 7.2 \cdot 10^{14}$ n_{eq}/cm^2 (see Table 1) with 24 GeV/c proton, was later irradiated also with neutrons in the TRIGA reactor in Ljubljana [17, 18] to $\Phi_{eq} \sim 8.8 \cdot 10^{14}$ n_{eq}/cm^2. This resulted in a mixture close to the expected at the most exposed part of ITk strips. After irradiation with protons the sample was kept in the freezer. During irradiation with neutrons the time without cooling was only few minutes so there was no significant annealing of damage caused by proton irradiation. Charge collection measured with ^{90}Sr after annealing for 80 minutes at 60°C
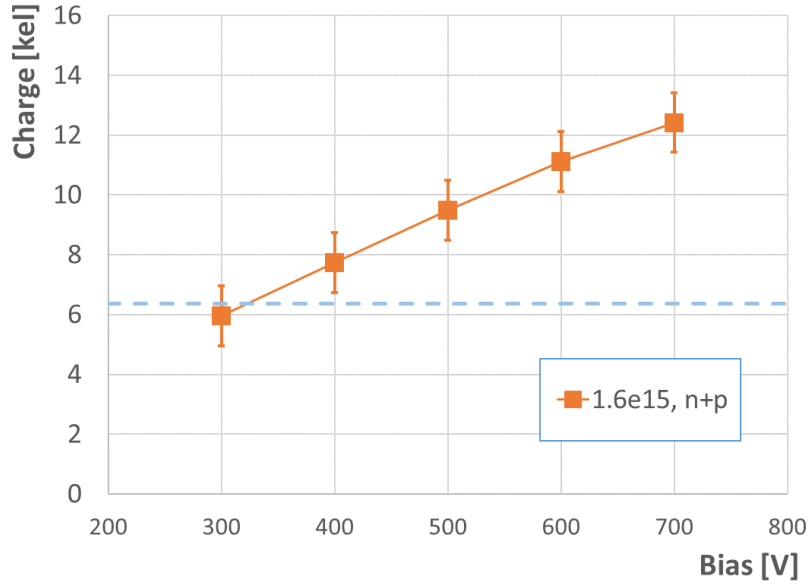
Figure 8: Collected charge vs. bias voltage for mini strip detector irradiated with 24 GeV/c protons to $\Phi_{eq} \sim 7.2 \cdot 10^{14}$ n_{eq}/cm^2 and with reactor neutrons to $\Phi_{eq} \sim 8.8 \cdot 10^{14}$ n_{eq}/cm^2, total fluence $\Phi_{eq} \sim 1.6 \cdot 10^{15}$ n_{eq}/cm^2.

as a function of bias voltage is shown in Fig. 8. It can be seen that collected charge at 500 V is higher than 6350 electrons, which is the minimum required

for strip detectors in the ITk.
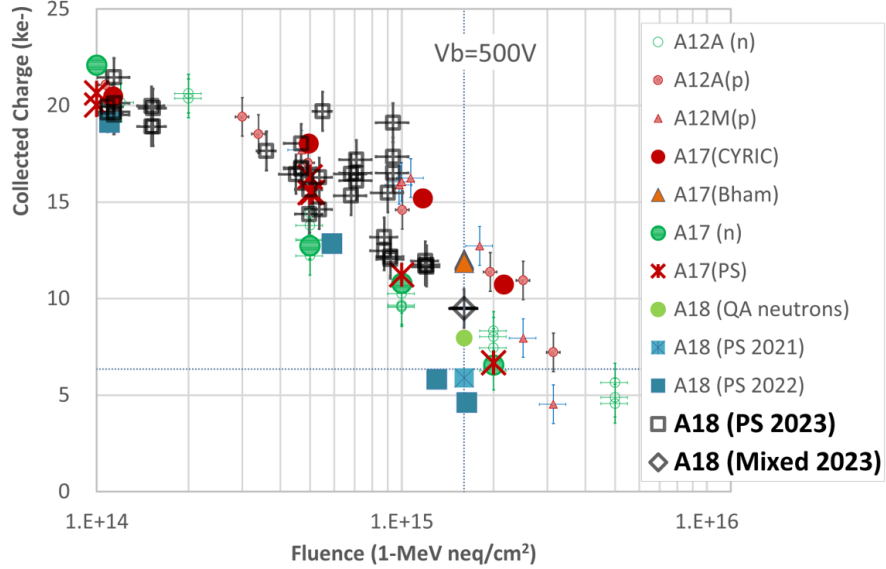
6. Conclusion

Figure 9: Collected charge at 500 V bias vs. fluence. The graph shows a collection of results from various irradiation tests with neutrons (n in the legend), low energy protons (p, CYRIC, Bham) and with 24 GeV/c protons (PS) [15]. Measurements from irradiation experiment described here are marked with A18(PS 2023) and A18(Mixed 2023).

Figure 9 shows comparison of charge collection measurements as function of fluence from large number of irradiations with different particles and different versions of strip detectors including measurements after irradiations with 24 GeV/c protons, in which collected charge below the acceptance level of 6350 electrons was measured near the design fluence of $\Phi_{eq} = 1.6 \cdot 10^{15}$ n_{eq}/cm^2 (symbols A18 (PS2021) and A18 (PS2022) in Fig. 9). These measurements motivated irradiation experiment described in this work to find

explanations for the low collected charge and to assure that charge collection will be sufficient up to highest fluences.

Dosimetry with Al foils and Geant4 simulation confirm that effects of irradiation angles and scattering material between the beam and the samples, which are specific to the sample holders, have to be considered to correctly estimate the fluence to which the samples were exposed in the narrow beam at CERN PS. This was not done in measurements that resulted in charge collection below the acceptance level. Actual fluence in those measurements might have been underestimated by up to 60% which resulted in low charge collection efficiency.

Measurements presented in this work including the results after irradiation with combination of protons and neutrons give a strong confirmation that the collected charges are well above the acceptance level and that the strip detectors in ATLAS ITk are sufficiently radiation hard for successful operation up to the highest fluences expected at HL-LHC.

7. Acknowledgments

References

[1] ATLAS Collaboration, The ATLAS experiment at the CERN large hadron collider, JINST 3 (2008) S08003. `doi:http://dx.doi.org/10.1088/1748-0221/3/08/S08003`.

[2] ATLAS Collaboration, TDR for the ATLAS Inner Tracker Strip Detector, CERN-LHCC-2017-005 (2017) ATLAS–TDR–025`doi:https://cds.cern.ch/record/2257755`.

[3] E. Bach et al., Analysis of the quality assurance results from the initial part of production of the ATLAS18 ITK strip sensors, Nucl. Instr. and Meth. A 1064 (2024) 169435. `doi:10.1016/j.nima.2024.169435`.

[4] F. Ravotti et al., A New High-intensity Proton Irradiation Facility at the CERN PS East Area, Proceedings of TIPP 2014 PS(TIPP2014) (2024) 354. `doi:10.22323/1.213.0354`.

[5] F. Ravotti et al., The IRRAD Proton Irradiation Facility Control, Data Managment and Beam Diagnostic Systems: An Outlook of The

Major Upgrades Beyond The CERN Long Shutdown 2, Proceedings ICALEPCS2019, New York, NY, USA PS(TIPP2014) (2024) 354. `doi: 10.18429/JACoW-ICALEPCS2019-WEPHA127`.

[6] Y. Unno et al., Specifications and pre-production of n$^+$-in-p large-format strip sensors fabricated in 6-inch silicon wafers, ATLAS18, for the Inner Tracker of the ATLAS Detector for High-Luminosity Large Hadron Collider, JINST 18 (2023) T03008. `doi:10.1088/1748-0221/18/03/T03008`.

[7] S. Hirose et al., ATLAS ITk Strip Sensor Quality Assurance Tests and Results of ATLAS18 Pre-production Sensors, JPS Conf. Proc. of Vetex 2022 42 (2024) 011017. `doi:10.7566/JPSCP.42.011017`.

[8] M. Glaser, F. Ravotti, M. Moll , Dosimetry Assessments in the Irradiation Facilities at the CERN-PS Accelerator, IEEE Trans. Nucl. Sci. 53 (2006) 2016. `doi:10.1109/TNS.2006.880569`.

[9] P. Allport et al., Experimental Determination of Proton Hardness Factors at Several Irradiation Facilities, JINST 14 (2019) P12004. `doi: 10.1088/1748-0221/14/12/P12004`.

[10] M. Moll, E. Fretwurst, G. Lindström, Leakage current of hadron irradiated silicon detectors – material dependence, Nucl. Instr. and Meth. A 426 (1999) 87. `doi:10.1016/S0168-9002(98)01475-2`.

[11] S. Agostinelli et al., GEANT4 – a simulation toolkit, Nucl. Instr. and Meth. A 506 (3) (2003) 250–303. `doi:10.1016/S0168-9002(03)01368-8`.

[12] The Shielding physics list. doi:https://geant4.web.cern.ch/documentation/dev/plg_html/PhysicsListGuide/reference_PL/Shielding.html.

[13] J. Bernabeu et al., ALIBAVA Silicon Microstrip Readout System for Educational Purposes, Nucl. Part. Phys. Proc. 273-275 (2016) 2563–2565. doi:10.1016/j.nuclphysbps.2015.09.460.

[14] K. Hara et al., Charge collection and field profile studies of heavily irradiated strip sensors for the ATLAS inner tracker upgrade, Nucl. Instr. and Meth. A 831 (2016) 181–188. doi:10.1016/j.nima.2016.04.035.

[15] K. Hara et al., Charge collection study with the ATLAS ITk prototype silicon strip sensors ATLAS17LS, Nucl. Instr. and Meth. A 983 (2020) 164422. doi:10.1016/j.nima.2020.164422.

[16] V. Cindro et al., Measurement of the charge collection in irradiated miniature sensors for the upgrade of the ATLAS phase-II strip tracker, Nucl. Instr. and Meth. A 924 (2019) 153. doi:10.1016/j.nima.2018.10.007.

[17] L. Snoj, G. Žerovnik and A. Trkov, Computational analysis of irradiation facilities at the JSI TRIGA reactor Measurement, Appl. Radiat. Isot. 70 (2012) 483. doi:10.1016/j.apradiso.2011.11.042.

[18] K. Ambrožič, G. Žerovnik, L. Snoj, Computational analysis of dose rates at the JSI TRIGA reactor irradiation facilities, Appl. Radiat. Isot. 130 (2017) 140. doi:10.1016/j.apradiso.2017.09.022.